J. math. fluid mech. 2 (2000) 126–150
1422-6928/00/020126-25 $ 1.50+0.20/0

Journal of Mathematical Fluid Mechanics

Multimodels for Incompressible Flows

Lorella Fatone, Paola Gervasio and Alfio Quarteroni

Abstract. The Navier–Stokes equations for incompressible fluids are coupled to models of reduced complexity, such as Oseen and Stokes, and the corresponding transmission conditions are investigated. A mathematical analysis of the corresponding problems is carried out. Numerical results obtained by finite elements and spectral elements are shown on several flow fields of physical interest.

Mathematics Subject Classification (2000). 76D05, 65M55, 65M60, 65M70.

Keywords. Navier–Stokes equations, domain decomposition methods, finite elements, spectral element methods, far-field boundary treatment.

1. Introduction

Navier–Stokes equations provide the mathematical model to describe the motion of incompressible viscous fluids. Their numerical approximation is in general rather difficult due, from one hand, to the coupling between velocity and pressure fields, and, from the other hand, to the presence of the non-linear convective term.

Simplified, linear models are frequently used in the numerical literature with the aim of alleviating the complexity that arises from the non linearity. Relevant examples are represented by the Stokes equations (which corresponds to drop the non-linear term) and the Oseen equations (corresponding to setting the convective velocity equals to a constant field). In special circumstances, the above simplified models provide reasonably accurate solutions.

In this paper we propose hybrid (or, more precisely, *heterogeneous*) models that couple the original Navier–Stokes equations with a simplified system that can be reasonably adopted in a given subregion of the computational domain.

This approach is motivated primarily by the need of reducing the overall complexity of the numerical method. However, its use can be justified only in those situations where the difference between the solution of the heterogeneous problem

This research has been carried out with the support of M.U.R.S.T., 1998 "Metodologie Numeriche Avanzate per il Calcolo Scientifico" and Swiss National Science Foundation Project N. 21-54139.98.

and that of the full Navier–Stokes problem is "acceptably small".

From the mathematical standpoint, this heterogeneous approach relies on a convenient set of matching conditions at the interface separating the two subregions, say Ω_1 and Ω_2, where the Navier–Stokes equations and the linear equations are, respectively, adopted. The analysis of these interface conditions is carried out in this paper. It reconsiders and generalises a similar analysis that was previously made by Feistauer and Schwab in [4], [3], [5] for the solution of flow equations in exterior domains.

Heterogeneous couplings in the context of other fluid flow problems were formerly considered, see e.g. [13], Ch. 8, and the references therein.

Another mathematical aspect that has to be faced is the development of suitable iterative algorithms that allow the use of independent solvers in each subregion, and their convergence analysis. This issue will be addressed in [2].

This paper contains a validation and assessment of the proposed model on three different test cases of physical interest: steady flow in a channel with a backward facing step, unsteady flow past a cylinder in a channel, and unsteady flow past a cylinder in a circular domain.

For the numerical approximation we consider both the high order spectral element method (see, e.g. [8], [9]) and the finite element method.

An extensive comparative analysis is carried out, and the results substantiate the interest of the proposed heterogeneous approaches.

An outline of this paper is as follows: in Section 2 we motivate our investigation by considering several potential fields of application. In Section 3 we consider some coupled models for incompressible viscous flows, determining, in particular, the mathematically admissible transmission conditions at subdomain interfaces and analysing the well-posedness of the coupled problems. Finally, in Section 4 we show the numerical results obtained on the above mentioned test cases.

2. Heterogeneous couplings: motivations

Before addressing the issue of heterogeneous coupling, we briefly review the following three models: Navier–Stokes, Oseen and Stokes equations.

The Navier–Stokes problem for viscous incompressible flows reads: find a velocity vector field $\mathbf{u} = \mathbf{u}(\mathbf{x}, t)$ and a pressure scalar field $p = p(\mathbf{x}, t)$ such that

$$\frac{\partial \mathbf{u}}{\partial t} - \nu \Delta \mathbf{u} + \nabla p = \mathbf{f} - (\mathbf{u} \cdot \nabla)\mathbf{u} \text{ in } \Omega \times (0, T) \tag{1}$$

$$\nabla \cdot \mathbf{u} = 0 \qquad \text{in } \Omega \times (0, T) \tag{2}$$

plus suitable boundary and initial conditions, where Ω is a bounded domain in $\mathbb{R}^d$ ($d = 2, 3$) with a Lipschitz continuous boundary $\partial\Omega$, $T > 0$, $\mathbf{f}$ is a given vector field and $\nu = const. > 0$ is the viscosity.

The Oseen equations are obtained from (1)–(2) replacing the momentum equa-

tion (1) by

$$\frac{\partial \mathbf{u}}{\partial t} - \nu \Delta \mathbf{u} + \nabla p = \mathbf{f} - (\mathbf{u}_\infty \cdot \nabla)\mathbf{u} \qquad \text{in } \Omega \times (0,T), \tag{3}$$

where $\mathbf{u}_\infty$ is a prescribed solenoidal vector field. Although in the classical Oseen model $\mathbf{u}_\infty$ plays the role of a *constant* farfield velocity, we will refer to (3), (2) as to an Oseen problem, even when the prescribed solenoidal field $\mathbf{u}_\infty$ is *not constant*.

In the special case in which $\mathbf{u}_\infty = \mathbf{0}$, we obtain the Stokes problem, that is given by equation (2) and the linear momentum equation

$$\frac{\partial \mathbf{u}}{\partial t} - \nu \Delta \mathbf{u} + \nabla p = \mathbf{f} \qquad \text{in } \Omega \times (0,T). \tag{4}$$

Both Oseen and Stokes equations can be regarded as simplified versions of Navier–Stokes equations.

Equations (1), (3) and (4) may all be regarded as special case of

$$\frac{\partial \mathbf{u}}{\partial t} - \nu \Delta \mathbf{u} + \nabla p = \mathbf{f} - (\mathbf{w} \cdot \nabla)\mathbf{u} \qquad \text{in } \Omega \times (0,T), \tag{5}$$

with $\mathbf{w} = \mathbf{u}$, $\mathbf{w} = \mathbf{u}_\infty$ and $\mathbf{w} = \mathbf{0}$, respectively.

There are cases in which it might be convenient to solve the Navier–Stokes equations (1)–(2) only in a subset (say Ω_1) of the computational domain Ω while using a reduced simplified model (like (4), (2) or (3), (2)) in the remainder Ω_2 of the domain itself.

In general, we will have $\overline{\Omega} = \overline{\Omega}_1 \cup \overline{\Omega}_2$ and $\Gamma := \partial\Omega_1 \cap \partial\Omega_2$ will denote the interface between Ω_1 and Ω_2.

If $\mathbf{w}_i$ denotes the restriction of $\mathbf{w}$ to Ω_i, $i = 1, 2$, in those case we are therefore interested to solve (5) where we take

$$\mathbf{w}_1 = \mathbf{u}_{|\Omega_1} \quad \text{and} \quad \mathbf{w}_2 \text{ is equal either to } \mathbf{u}_{\infty|\Omega_2} \text{ or to } \mathbf{0}. \tag{6}$$

Note that the vector field $\mathbf{w}$ can be discontinuous across the subdomains interface Γ.

The system given by (5), (2) with $\mathbf{w}$ defined as in (6) plus suitable boundary and initial conditions, characterises a *multifield* problem. The choice $\mathbf{w}_1 = \mathbf{u}_1$ and $\mathbf{w}_2 = \mathbf{0}$ corresponds to a *Navier–Stokes/Stokes* coupling, while the choice $\mathbf{w}_1 = \mathbf{u}_1$ and $\mathbf{w}_2 = \mathbf{u}_{\infty|\Omega_2}$ corresponds to a *Navier–Stokes/Oseen* coupling.

More precisely, the multi-domain formulation that we will consider is: find $\mathbf{u}_i$ and p_i, $i = 1, 2$ satisfying

$$\frac{\partial \mathbf{u}_i}{\partial t} - \nu \Delta \mathbf{u}_i + \nabla p_i = \mathbf{f} - (\mathbf{w}_i \cdot \nabla)\mathbf{u}_i \qquad \text{in } \Omega_i \times (0,T) \;\; i = 1,2 \tag{7}$$

$$\nabla \cdot \mathbf{u}_i = 0 \qquad \text{in } \Omega_i \times (0,T) \;\; i = 1,2 \tag{8}$$

$$\mathbf{u}_1 = \mathbf{u}_2 \qquad \text{on } \Gamma \times (0,T) \tag{9}$$

$$-p_1\mathbf{n} + \nu(\mathbf{n} \cdot \nabla)\mathbf{u}_1 = -p_2\mathbf{n} + \nu(\mathbf{n} \cdot \nabla)\mathbf{u}_2 \quad \text{on } \Gamma \times (0,T) \tag{10}$$

where $\mathbf{u}_i = \mathbf{u}_{|\Omega_i}$, $p_i = p_{|\Omega_i}$ for $i = 1, 2$, and $\mathbf{n}$ denotes the normal unit vector on Γ directed from Ω_1 to Ω_2.

Conditions (9)–(10) are called *transmission conditions* and ensure the continuity of the velocity field and the continuity of the "flux" across the interface, respectively.

For the Navier–Stokes/Oseen coupling, the transmission condition (10) can be replaced by the following one (see [3]):

$$\begin{aligned} &-p_1\mathbf{n}+\nu(\mathbf{n}\cdot\nabla)\mathbf{u}_1-\frac{1}{2}(\mathbf{w}_1\cdot\mathbf{n})\mathbf{u}_1 \\ &\quad=-p_2\mathbf{n}+\nu(\mathbf{n}\cdot\nabla)\mathbf{u}_2-\frac{1}{2}(\mathbf{w}_2\cdot\mathbf{n})\mathbf{u}_2 \qquad \text{on } \Gamma\times(0,T). \end{aligned} \tag{11}$$

In Section 3.1 we will see that this condition is associated to a different treatment of the convective term.

Besides, from now on, given a sufficiently regular vector field $\mathbf{w}$, we set:

$$\begin{aligned} &T_S(\mathbf{u},p)\mathbf{n}=-p\mathbf{n}+\nu(\mathbf{n}\cdot\nabla)\mathbf{u} \qquad (Stokes\ flux), \\ &T_O(\mathbf{w};\mathbf{u},p)\mathbf{n}=-p\mathbf{n}+\nu(\mathbf{n}\cdot\nabla)\mathbf{u}-\frac{1}{2}(\mathbf{w}\cdot\mathbf{n})\mathbf{u} \quad (Oseen\ flux). \end{aligned} \tag{12}$$

In the following sections we will provide a mathematical justification for the use of either (10) or (11).

2.1. Time differentiation and coupling

In order to analyse the impact of time differentiation on our multifield models, let $\Delta t\in(0,T)$ be a time step; we set $t^0=0$ and $t^n=n\cdot\Delta t$, with $n=1,\dots,M$ and M denoting the integral part of $T/\Delta t$. We consider, for instance, the Euler semi-implicit finite difference scheme ([15], Ch. III, § 5), for the time-approximation of (7)–(10). The problem reads: given $\mathbf{u}^n$, for $n\geq 0$, find the solution $(\mathbf{u}^{n+1},p^{n+1})$ of the system:

$$\frac{(\mathbf{u}_i^{n+1}-\mathbf{u}_i^n)}{\Delta t}-\nu\Delta\mathbf{u}_i^{n+1}+\nabla p_i^{n+1}=\mathbf{f}^{n+1}-(\mathbf{w}_i^n\cdot\nabla)\mathbf{u}_i^{n+1} \text{ in } \Omega_i \ i=1,2 \tag{13}$$

$$\nabla\cdot\mathbf{u}_i^{n+1}=0 \qquad \text{in } \Omega_i \ i=1,2 \tag{14}$$

with

$$\mathbf{u}_1^{n+1}=\mathbf{u}_2^{n+1} \text{ on } \Gamma \tag{15}$$

and either

$$T_S(\mathbf{u}_1^{n+1},p_1^{n+1})\mathbf{n}=T_S(\mathbf{u}_2^{n+1},p_2^{n+1})\mathbf{n} \text{ on } \Gamma \tag{16}$$

or

$$T_O(\mathbf{w}_1^n;\mathbf{u}_1^{n+1},p_1^{n+1})\mathbf{n}=T_O(\mathbf{w}_2^n;\mathbf{u}_2^{n+1},p_2^{n+1})\mathbf{n} \text{ on } \Gamma. \tag{17}$$

In that case, $\mathbf{w}_1^n=\mathbf{u}_1^n$, while $\mathbf{w}_2^n$ can be either $\mathbf{u}_{\infty|\Omega_2}$ or $\mathbf{0}$. We observe that this problem yields either an Oseen/Oseen coupling or an Oseen/Stokes coupling depending on the choice that is made for $\mathbf{w}_2^n$.

We point out that a Navier–Stokes/Stokes or, even better, a Navier–Stokes/Oseen coupling may arise when we consider perturbed and unperturbed flow regions due to the presence of bodies or obstacles, or when we want to handle in an efficient way far field boundary conditions (see Section 4). The use of different time-advancing schemes to accommodate different local velocity fields, leads instead to an Oseen/Stokes coupling (see Section 4).

Indeed, if the velocity field varies substantially through the computational domain, one might be led to consider two different schemes for time-integration, characterised by a semi-implicit or fully explicit treatment of the convective term. A semi-implicit scheme, that has a weak (or no) stability restriction on the time-step, could be used in the subregion of Ω where $|\mathbf{u}(\mathbf{x})|$ attains the largest values, while an explicit scheme, that entails a more restrictive stability condition, could be used elsewhere.

Precisely, should a condition like

$$\|\mathbf{u}_1\|_{L^\infty(\Omega_1)} >> \|\mathbf{u}_2\|_{L^\infty(\Omega_2)} \tag{18}$$

hold for two different subsets Ω_1 and Ω_2 of the domain Ω, the momentum equation (13) could be replaced by:

$$\begin{aligned} &\frac{1}{\Delta t_i}(\mathbf{u}_i^{n+1} - \mathbf{u}_i^n) - \nu\Delta\mathbf{u}_i^{n+1} + (\mathbf{w}_i^n \cdot \nabla)\mathbf{u}_i^{n+\alpha} + \nabla p_i^{n+1} \\ &\quad = \mathbf{f}^{n+1} \qquad \text{in } \Omega_i, \quad i = 1, 2 \end{aligned} \tag{19}$$

with $\alpha = 1$ in Ω_1 and $\alpha = 0$ in Ω_2.

Hence, the Euler semi-implicit scheme in Ω_1, that is *unconditionally stable* (see [15]), corresponding to $\alpha = 1$, is used in Ω_1 whereas the explicit treatment of the convective term in Ω_2, corresponding to $\alpha = 0$, entails a CFL stability condition that reads

$$\Delta t \leq \frac{C_2 h}{\|\mathbf{u}_2\|_{L^\infty(\Omega_2)}}, \tag{20}$$

where h is the smallest space-discretisation grid-size.

3. The models for incompressible flows

In this section we refer to a steady problem, like the one (19) that is obtained after time-discretisation of the time-dependent Navier–Stokes equations. For the mathematical analysis of flow equations in bounded and exterior domains we refer, e.g., to [15], [6], [7], [11].

3.1. The differential problems and their weak formulations

Given a vector field $\mathbf{f} : \Omega \to \mathbb{R}^2$, we consider the following stationary problem: find $\mathbf{u} : \Omega \to \mathbb{R}^2$ and $p : \Omega \to \mathbb{R}$ such that

$$\begin{cases} \alpha\mathbf{u} - \nu\Delta\mathbf{u} + \nabla p = \mathbf{f} - (\mathbf{w}\cdot\nabla)\mathbf{u} & \text{in } \Omega \\ \nabla\cdot\mathbf{u} = 0 & \text{in } \Omega \\ \mathbf{u} = \mathbf{0} & \text{on } \partial\Omega_D \\ T_S(\mathbf{u},p)\mathbf{n} = \mathbf{0} & \text{on } \partial\Omega_N \end{cases} \tag{21}$$

where $\partial\Omega_D$ and $\partial\Omega_N$ are two disjoint subsets of $\partial\Omega$ such that $\overline{\partial\Omega} = \overline{\partial\Omega}_D \cup \overline{\partial\Omega}_N$, T_S is the stress tensor defined in (12), $\mathbf{n}$ is the outward unit normal vector to Ω and typically $\alpha = c/\Delta t$, where $c > 0$ depends on the time-differentiation scheme that is used.

The vector field $\mathbf{w}$ can be given as data (in which case (21) is a linear problem), or it could be defined as in (6). Note that, whatever case is considered, the vector field $\mathbf{w}$ is not necessarily continuous across Γ. In general, we suppose that $\mathbf{w}$ belongs to the following space

$$\mathbf{W} := \{\mathbf{w} \in [L^\infty(\Omega)]^2 :\ \mathbf{w}_{|\Omega_i} \in [H^1(\Omega_i)]^2 \text{ and } \nabla\cdot\mathbf{w}_{|\Omega_i} = 0 \text{ for } i = 1,2\}. \tag{22}$$

In order to analyse the well-posedness of (21), let us introduce the following functional spaces:

$$H^1_{\partial\Omega_D}(\Omega) = \{v \in H^1(\Omega) :\ v_{|\partial\Omega_D} = 0\},\ \ \mathbf{V} = [H^1_{\partial\Omega_D}(\Omega)]^2, \quad \text{and } Q = L^2(\Omega). \tag{23}$$

In the special case when $\partial\Omega_D \equiv \partial\Omega$, we choose instead

$$\mathbf{V} = [H^1_0(\Omega)]^2 \quad \text{and} \quad Q = L^2_0(\Omega) = \left\{ q \in L^2(\Omega) :\ \int_\Omega q \mathrm{d}\Omega = 0 \right\}. \tag{24}$$

Given $\mathbf{f} \in [L^2(\Omega)]^2$, a weak formulation of problem (21) reads: find $\mathbf{u} \in \mathbf{V}$ and $p \in Q$ such that

$$\begin{cases} (\alpha\mathbf{u},\mathbf{v})_\Omega + \nu(\nabla\mathbf{u},\nabla\mathbf{v})_\Omega - (p,\nabla\cdot\mathbf{v})_\Omega = (\mathbf{f},\mathbf{v})_\Omega - ((\mathbf{w}\cdot\nabla)\mathbf{u},\mathbf{v})_\Omega & \forall\mathbf{v}\in\mathbf{V} \\ (\nabla\cdot\mathbf{u},q)_\Omega = 0 & \forall q \in Q, \end{cases} \tag{25}$$

where $(\cdot,\cdot)_\Omega$ denotes the inner product in $L^2(\Omega)$.

An alternative weak form reads: find $\mathbf{u} \in \mathbf{V}$ and $p \in Q$ such that

$$\begin{cases} (\alpha\mathbf{u},\mathbf{v})_\Omega + \nu(\nabla\mathbf{u},\nabla\mathbf{v})_\Omega - (p,\nabla\cdot\mathbf{v})_\Omega \\ \qquad = (\mathbf{f},\mathbf{v})_\Omega - ((\mathbf{w}\cdot\nabla)\mathbf{u},\mathbf{v})_\Omega - \dfrac{1}{2}(([\mathbf{w}]\cdot\mathbf{n})\mathbf{u}_{|\Gamma},\mathbf{v}_{|\Gamma})_\Gamma & \forall\mathbf{v}\in\mathbf{V} \\ (\nabla\cdot\mathbf{u},q)_\Omega = 0 & \forall q \in Q, \end{cases} \tag{26}$$

being $(\cdot,\cdot)_\Gamma$ the L^2 inner product on Γ and having denoted by $[\,\cdot\,]$ the jump on Γ. Precisely

$$[\mathbf{w}] := \lim_{h\to 0^+} \mathbf{w}(\mathbf{x} + h\mathbf{n}(\mathbf{x})) - \lim_{h\to 0^-} \mathbf{w}(\mathbf{x} + h\mathbf{n}(\mathbf{x})) \quad \forall\mathbf{x}\in\Gamma. \tag{27}$$

Here and in the sequel the restrictions $\mathbf{v}_{|\partial\Omega_N}, \mathbf{v}_{|\Gamma}$, etc. will be understood in the sense of the traces (see, e.g. [10]).

Indeed, (26) is the variational formulation associated to a problem like (21) where the momentum equation is modified as follows:

$$\alpha\mathbf{u} - \nu\Delta\mathbf{u} + \nabla p = \mathbf{f} - (\mathbf{w}\cdot\nabla)\mathbf{u} - \gamma(\mathbf{u}) \quad \text{in } \Omega, \tag{28}$$

where $\gamma : \mathbf{V} \to \mathbf{V}'$ is defined as follows

$$\underset{\mathbf{V}'}{\langle \gamma(\mathbf{u}), \mathbf{v}\rangle}_{\mathbf{V}} = \frac{1}{2}(([\mathbf{w}]\cdot\mathbf{n})\mathbf{u}_{|\Gamma}, \mathbf{v}_{|\Gamma})_\Gamma \qquad \forall \mathbf{v} \in \mathbf{V}. \tag{29}$$

We note that (29) is well defined even if Γ is not smooth, but only Lipschitz continuous (see [1]).

Since

$$((\mathbf{w}\cdot\nabla)\mathbf{u}, \mathbf{v})_\Omega = \frac{1}{2}((\mathbf{w}\cdot\nabla)\mathbf{u}, \mathbf{v})_\Omega + \frac{1}{2}\sum_{i=1}^{2}((\mathbf{w}_{|\Omega_i}\cdot\nabla)\mathbf{u}_{|\Omega_i}, \mathbf{v}_{|\Omega_i})_{\Omega_i} \tag{30}$$

applying Green's formula, it is easy to see that problem (26) is equivalent to find $\mathbf{u} \in \mathbf{V}$ and $p \in Q$ such that

$$\begin{cases} (\alpha\mathbf{u}, \mathbf{v})_\Omega + \nu(\nabla\mathbf{u}, \nabla\mathbf{v})_\Omega - (p, \nabla\cdot\mathbf{v})_\Omega \\ \qquad = (\mathbf{f}, \mathbf{v})_\Omega - \frac{1}{2}((\mathbf{w}\cdot\nabla)\mathbf{u}, \mathbf{v})_\Omega + \frac{1}{2}((\mathbf{w}\cdot\nabla)\mathbf{v}, \mathbf{u})_\Omega \ \ \forall \mathbf{v} \in \mathbf{V} \\ (\nabla\cdot\mathbf{u}, q)_\Omega = 0 \qquad\qquad \forall q \in Q. \end{cases} \tag{31}$$

3.2. Existence and uniqueness results

Let us introduce the following trilinear forms defined on $\mathbf{W}\times\mathbf{V}\times\mathbf{V}$:

$$c(\mathbf{w}; \mathbf{u}, \mathbf{v}) = (\alpha\mathbf{u}, \mathbf{v})_\Omega + \nu(\nabla\mathbf{u}, \nabla\mathbf{v})_\Omega + ((\mathbf{w}\cdot\nabla)\mathbf{u}, \mathbf{v})_\Omega, \tag{32}$$

$$\begin{aligned} d(\mathbf{w}; \mathbf{u}, \mathbf{v}) = {} & (\alpha\mathbf{u}, \mathbf{v})_\Omega + \nu(\nabla\mathbf{u}, \nabla\mathbf{v})_\Omega + ((\mathbf{w}\cdot\nabla)\mathbf{u}, \mathbf{v})_\Omega \\ & + \frac{1}{2}(([\mathbf{w}]\cdot\mathbf{n})\mathbf{u}_{|\Gamma}, \mathbf{v}_{|\Gamma})_\Gamma. \end{aligned} \tag{33}$$

We also define the linear functional

$$\mathcal{F} : \mathbf{V} \to \mathbb{R} : \ \mathcal{F}(\mathbf{v}) = (\mathbf{f}, \mathbf{v})_\Omega, \tag{34}$$

and the bilinear form

$$b : \mathbf{V}\times Q \to \mathbb{R} : \ b(\mathbf{u}, q) = -(\nabla\cdot\mathbf{u}, q)_\Omega. \tag{35}$$

We have the following result concerning problem (25) for the case when $\mathbf{w}$ is given independently of $\mathbf{u}$.

Theorem 3.1. *Let $\mathbf{f} \in [L^2(\Omega)]^2$ and $\mathbf{w} \in \mathbf{W}$ be given vector fields. If either one of the following conditions is satisfied:*

$$\alpha \geq 0 \text{ a.e. in } \Omega \text{ and } [\mathbf{w}] \cdot \mathbf{n} \leq 0 \text{ on } \Gamma, \tag{36}$$

$$\inf_{\Omega} \alpha - \frac{1}{2\nu} \|\mathbf{w}\|^2_{\infty,\Omega} \geq 0 \text{ in } \Omega, \tag{37}$$

then there exists a unique solution $(\mathbf{u}, p)$ to the linear problem (25).

Proof. The trilinear form (32) is continuous. The coercivity of $c(\cdot;\cdot,\cdot)$ follows from (36) or (37). In fact, since that $\nabla \cdot \mathbf{w}_{|\Omega_i} = 0$, for $i = 1, 2$, by Green's formula we have:

$$\begin{aligned} c(\mathbf{w};\mathbf{u},\mathbf{u}) &= \int_{\Omega} \alpha \mathbf{u}^2 \mathrm{d}\Omega + \nu \int_{\Omega} |\nabla \mathbf{u}|^2 \mathrm{d}\Omega + \frac{1}{2} \sum_{i=1}^{2} \int_{\Omega_i} \mathbf{w}_{|\Omega_i} \cdot \nabla(|\mathbf{u}|^2) \mathrm{d}\Omega_i \\ &= \int_{\Omega} \alpha \mathbf{u}^2 \mathrm{d}\Omega + \nu \int_{\Omega} |\nabla \mathbf{u}|^2 \mathrm{d}\Omega - \frac{1}{2} \int_{\Gamma} ([\mathbf{w}] \cdot \mathbf{n}) |\mathbf{u}_{|\Gamma}|^2 \mathrm{d}\Gamma \end{aligned} \tag{38}$$

hence $c(\cdot;\cdot,\cdot)$ is coercive by (36).

Otherwise, when we apply the Young inequality to $((\mathbf{w}\cdot\nabla)\mathbf{u}, \mathbf{u})_{\Omega}$, the coercivity of $c(\cdot;\cdot,\cdot)$ is ensured by (37).

The form $b(\cdot,\cdot)$ (defined in (35)) is continuous and it satisfies the following inf-sup condition (see [13], Prop. 5.3.2): there exists a constant $\beta > 0$ such that

$$\forall\, q \in Q\ \exists\, \mathbf{v} \in [H^1_{\Omega_D}(\Omega)]^2\ ,\ \mathbf{v} \neq \mathbf{0}\ :\ b(\mathbf{v}, q) \geq \beta ||\mathbf{v}||_{H^1(\Omega)} ||q||_{L^2(\Omega)}. \tag{39}$$

Applying now an abstract result on saddle point problems ([12], Thm 7.4.1) the thesis follows. □

A similar result can be proven for problem (26) (or equivalently for problem (31)), for which the existence and uniqueness of the solution is ensured under the unique assumption $\alpha \geq 0$ a.e. in Ω. In particular the following theorem, whose proof is omitted for sake of brevity, holds:

Theorem 3.2. *Given $\mathbf{f} \in [L^2(\Omega)]^2$ and $\mathbf{w} \in \mathbf{W}$, if*

$$\alpha \geq 0 \text{ a.e. in } \Omega, \tag{40}$$

then there exists a unique solution $(\mathbf{u}, p)$ to (26) (or equivalently to (31)).

Remark 3.1. The existence of a weak solution for problem (26) (or equivalently (31)), in the case in which $\mathbf{w}$ is chosen as in (6), is a consequence of a result of Feistauer and Schwab (see [3], Thm 3.1 where Ω_n has to be replaced by the domain Ω). An alternative proof based on a multi-domain argument is given in [2].

3.3. The multi-domain formulations

The stationary multi-domain problem which corresponds to (21) reads: find $\mathbf{u}_i : \Omega_i \to \mathbb{R}^2$ and $p_i : \Omega_i \to \mathbb{R},\ i = 1, 2$ such that for $i = 1, 2$:

$$\begin{cases} \alpha\mathbf{u}_i - \nu\Delta\mathbf{u}_i + \nabla p_i = \mathbf{f} - (\mathbf{w}_i \cdot \nabla)\mathbf{u}_i & \text{in } \Omega_i \\ \nabla \cdot \mathbf{u}_i = 0 & \text{in } \Omega_i \\ \mathbf{u}_i = \mathbf{0} & \text{on } \partial\Omega_i \cap \partial\Omega_D \\ T_S(\mathbf{u}_i, p_i)\mathbf{n}_i = \mathbf{0} & \text{on } \partial\Omega_i \cap \partial\Omega_N \end{cases} \tag{41}$$

with transmission conditions (9) and (10). To avoid unnecessary technical difficulties, we suppose that the decomposition of Ω is chosen in such a way that $\partial\Omega_i \cap \partial\Omega_N \neq \emptyset$, $i = 1, 2$. Under this assumption in fact, the boundary data need not verify any compatibility condition. However, when $\partial\Omega_N \equiv \emptyset$ similar arguments can be developed, see [13], Ch. 5.

The physical meaning of the split formulation (41) is clear as soon as the original solution of problem (21) is smooth enough. Otherwise, the equalities in Ω_i, $i = 1, 2$, hold in the sense of distributions, while those on Γ in the sense of the traces. In a more general framework, we resort to the weak formulation of both problems. To this aim we set

$$\begin{aligned} V_i &= \{v \in H^1(\Omega_i) :\ v_{|\partial\Omega_i \cap \partial\Omega_D} = 0\}\ , \quad i = 1, 2, \\ V_i^0 &= \{v \in H^1(\Omega_i) :\ v_{|\partial\Omega_i \setminus \partial\Omega_N} = 0\}\ , \quad i = 1, 2, \\ \Lambda &= \{\eta \in H^{1/2}(\Gamma) :\ \eta = v_{|\Gamma} \text{ for a suitable } v \in H^1_{\partial\Omega_D}(\Omega)\}. \end{aligned} \tag{42}$$

Then, for $i = 1, 2$ we define the extension operators:

$$\boldsymbol{\mathcal{R}}_i : [\Lambda]^2 \to [V_i]^2 :\quad (\boldsymbol{\mathcal{R}}_i\boldsymbol{\eta})_{|\Gamma} = \boldsymbol{\eta}. \tag{43}$$

The weak two-domain formulation of problem (25) is: find $\mathbf{u}_i \in [V_i]^2$ and $p_i \in L^2(\Omega_i)$, for $i = 1, 2$, such that

$$\begin{aligned} &(\alpha\mathbf{u}_i, \mathbf{v}_i)_{\Omega_i} + \nu(\nabla\mathbf{u}_i, \nabla\mathbf{v}_i)_{\Omega_i} - (p_i, \nabla \cdot \mathbf{v}_i)_{\Omega_i} \\ &\qquad = (\mathbf{f}, \mathbf{v}_i)_{\Omega_i} - ((\mathbf{w}_i \cdot \nabla)\mathbf{u}_i, \mathbf{v}_i)_{\Omega_i} \qquad \forall \mathbf{v}_i \in [V_i^0]^2, \quad i = 1, 2 \end{aligned} \tag{44}$$

$$(\nabla \cdot \mathbf{u}_i, q_i)_{\Omega_i} = 0 \qquad \forall q_i \in L^2(\Omega_i), \quad i = 1, 2 \tag{45}$$

$$\mathbf{u}_1 = \mathbf{u}_2 \qquad \text{on } \Gamma \tag{46}$$

$$\begin{aligned} &\sum_{i=1}^{2}\Big[(\alpha\mathbf{u}_i, \boldsymbol{\mathcal{R}}_i\boldsymbol{\eta})_{\Omega_i} + \nu(\nabla\mathbf{u}_i, \nabla\boldsymbol{\mathcal{R}}_i\boldsymbol{\eta})_{\Omega_i} \\ &\qquad -(p_i, \nabla \cdot \boldsymbol{\mathcal{R}}_i\boldsymbol{\eta})_{\Omega_i} + ((\mathbf{w}_i \cdot \nabla)\mathbf{u}_i, \boldsymbol{\mathcal{R}}_i\boldsymbol{\eta})_{\Omega_i}\Big] \\ &\qquad = \sum_{i=1}^{2}(\mathbf{f}, \boldsymbol{\mathcal{R}}_i\boldsymbol{\eta})_{\Omega_i} \qquad \forall \boldsymbol{\eta} \in [\Lambda]^2. \end{aligned} \tag{47}$$

The equation (47) is the weak counterpart of the transmission condition (10) and it guarantees the continuity of the Stokes flux across the interface Γ.

The multi-domain weak formulation corresponding to (26) is obtained in the same way, but now instead of (47) we have the interface equation

$$\sum_{i=1}^{2}\Big[(\alpha\mathbf{u}_i,\boldsymbol{\mathcal{R}}_i\boldsymbol{\eta})_{\Omega_i}+\nu(\nabla\mathbf{u}_i,\nabla\boldsymbol{\mathcal{R}}_i\boldsymbol{\eta})_{\Omega_i}-(p_i,\nabla\cdot\boldsymbol{\mathcal{R}}_i\boldsymbol{\eta})_{\Omega_i} \tag{48}$$
$$+((\mathbf{w}_i\cdot\nabla)\mathbf{u}_i,\boldsymbol{\mathcal{R}}_i\boldsymbol{\eta})_{\Omega_i}+\frac{1}{2}(([\mathbf{w}]\cdot\mathbf{n})\mathbf{u}_{i|\Gamma},\boldsymbol{\eta})_{\Gamma}\Big]=\sum_{i=1}^{2}(\mathbf{f},\boldsymbol{\mathcal{R}}_i\boldsymbol{\eta})_{\Omega_i}\ \forall\boldsymbol{\eta}\in[\Lambda]^2.$$

Analogously, the two-domain variational form associated to (31) can be written as problem (44)–(47), provided (44) is replaced by

$$(\alpha\mathbf{u}_i,\mathbf{v}_i)_{\Omega_i}+\nu(\nabla\mathbf{u}_i,\nabla\mathbf{v}_i)_{\Omega_i}-(p_i,\nabla\cdot\mathbf{v}_i)_{\Omega_i}=(\mathbf{f},\mathbf{v}_i)_{\Omega_i} \tag{49}$$
$$-\frac{1}{2}((\mathbf{w}_i\cdot\nabla)\mathbf{u}_i,\mathbf{v}_i)_{\Omega_i}+\frac{1}{2}((\mathbf{w}_i\cdot\nabla)\mathbf{v}_i,\mathbf{u}_i)_{\Omega_i}\qquad\forall\mathbf{v}_i\in[V_i^0]^2,\quad i=1,2$$

and (47) by

$$\sum_{i=1}^{2}\Big[(\alpha\mathbf{u}_i,\boldsymbol{\mathcal{R}}_i\boldsymbol{\eta})_{\Omega_i}+\nu(\nabla\mathbf{u}_i,\nabla\boldsymbol{\mathcal{R}}_i\boldsymbol{\eta})_{\Omega_i}-(p_i,\nabla\cdot\boldsymbol{\mathcal{R}}_i\boldsymbol{\eta})_{\Omega_i} \tag{50}$$
$$+\frac{1}{2}((\mathbf{w}\cdot\nabla)\mathbf{u}_i,\boldsymbol{\mathcal{R}}_i\boldsymbol{\eta})_{\Omega_i}-\frac{1}{2}((\mathbf{w}_i\cdot\nabla)\boldsymbol{\mathcal{R}}_i\boldsymbol{\eta},\mathbf{u}_i)_{\Omega_i}\Big]=\sum_{i=1}^{2}(\mathbf{f},\boldsymbol{\mathcal{R}}_i\boldsymbol{\eta})_{\Omega_i}\ \forall\boldsymbol{\eta}\in[\Lambda]^2.$$

The transmission conditions (48) and (50) correspond to (11) and they guarantee the continuity of the Oseen flux.

Remark 3.2. The inf-sup condition (39) yields a similar condition on Ω_i, for every $i=1,2$: there exists a constant $\beta_i>0$ such that:

$$\forall\ q\in L^2(\Omega_i)\ \exists\ \mathbf{v}\in[H^1_{\Omega_D}(\Omega_i)]^2\ ,\ \mathbf{v}\neq\mathbf{0}\ :\ b(\mathbf{v},q)\geq\beta_i||\mathbf{v}||_{H^1(\Omega_i)}||q||_{L^2(\Omega_i)}. \tag{51}$$

We can easily deduce that both problems in Ω_1 and Ω_2 have a unique solution.

3.4. Equivalence theorems between single-domain and multi-domain formulations

If the vector field $\mathbf{w}$ is continuous across Γ, then (25) is equivalent to (26), and consequently (44)–(47) is equivalent to (44)–(46), (48).

If $\mathbf{w}\equiv\mathbf{0}$ in Ω we obtain the Stokes problem, for which the proof of the equivalence between single and multidomain formulation can be found in [13].

More generally, we can prove the following equivalence theorems which hold for every given vector field $\mathbf{w}\in\mathbf{W}$, either continuous or discontinuous.

Theorem 3.3. *Problem* (25) *is equivalent to* (44)–(47)*, in the sense that* $\mathbf{u}_{|\Omega_i} = \mathbf{u}_i$ *and* $p_{|\Omega_i} = p_i$ *for* $i = 1, 2$.

Proof. Let us first check that any solution $(\mathbf{u}, p)$ to (25) is a solution to (44)–(47) as well. Setting $\mathbf{u}_i := \mathbf{u}_{|\Omega_i}$, $p_i := p_{|\Omega_i}$, $i = 1, 2$, we have that $\mathbf{u}_i \in [V_i]^2$, $p_i \in L^2(\Omega_i)$ and (44)–(46) are satisfied, considering the extension by zero of any local test in the complementary domain. Defining for each $\boldsymbol{\eta} \in [\Lambda]^2$ the vector function $\boldsymbol{\mathcal{R}\eta}$ as:

$$\boldsymbol{\mathcal{R}\eta} := \begin{cases} \boldsymbol{\mathcal{R}}_1\boldsymbol{\eta} \text{ in } \Omega_1 \\ \boldsymbol{\mathcal{R}}_2\boldsymbol{\eta} \text{ in } \Omega_2 \end{cases} \tag{52}$$

it follows that $\boldsymbol{\mathcal{R}\eta} \in H^1(\Omega)$ since $\boldsymbol{\mathcal{R}}_i\boldsymbol{\eta} \in H^1(\Omega_i)$ and the trace $\boldsymbol{\eta}$ on Γ is the same from both sides. Then (47) can be equivalently rewritten as:

$$(\alpha\mathbf{u}, \boldsymbol{\mathcal{R}\eta})_\Omega + \nu(\nabla\mathbf{u}, \nabla\boldsymbol{\mathcal{R}\eta})_\Omega - (p, \nabla\cdot\boldsymbol{\mathcal{R}\eta})_\Omega = (\mathbf{f}, \boldsymbol{\mathcal{R}\eta})_\Omega - ((\mathbf{w}\cdot\nabla)\mathbf{u}, \boldsymbol{\mathcal{R}\eta})_\Omega. \tag{53}$$

Since $\boldsymbol{\mathcal{R}\eta} \in \mathbf{V}$, the previous equation is a special case of the first equation in (25) that corresponds to the choice $\mathbf{v} = \boldsymbol{\mathcal{R}\eta}$.

Let now $(\mathbf{u}_i, p_i)$, $i = 1, 2$ be a solution of the multi-domain problem (44)–(47). We show that the functions $\mathbf{u}$ and p defined by

$$\mathbf{u} := \begin{cases} \mathbf{u}_1 \text{ in } \Omega_1 \\ \mathbf{u}_2 \text{ in } \Omega_2 \end{cases} \qquad p := \begin{cases} p_1 \text{ in } \Omega_1 \\ p_2 \text{ in } \Omega_2 \end{cases} \tag{54}$$

provide a solution of (25). We have that $\mathbf{u} \in [H^1_{\partial\Omega_D}(\Omega)]^2$ (since $\mathbf{u}_1 = \mathbf{u}_2$ on Γ) and $p \in L^2(\Omega)$. Then for every $\mathbf{v} \in [H^1_{\partial\Omega_D}(\Omega)]^2$ we set $\boldsymbol{\eta} := \mathbf{v}_{|\Gamma} \in [\Lambda]^2$ so that $\mathbf{z}_i := \mathbf{v}_{|\Omega_i} - \boldsymbol{\mathcal{R}}_i\boldsymbol{\eta} \in [V_i^0]^2$, $i = 1, 2$. Owing to (44)–(47) we have

$$\begin{aligned} &(\alpha\mathbf{u}, \mathbf{v})_\Omega + \nu(\nabla\mathbf{u}, \nabla\mathbf{v})_\Omega - (p, \nabla\cdot\mathbf{v})_\Omega + ((\mathbf{w}\cdot\nabla)\mathbf{u}, \mathbf{v})_\Omega \\ &= \sum_{i=1}^{2} [(\alpha\mathbf{u}_i, \mathbf{z}_i)_{\Omega_i} + \nu(\nabla\mathbf{u}_i, \nabla\mathbf{z}_i)_{\Omega_i} - (p_i, \nabla\cdot\mathbf{z}_i)_{\Omega_i} + ((\mathbf{w}\cdot\nabla)\mathbf{u}_i, \mathbf{z}_i)_{\Omega_i} \\ &\quad + (\alpha\mathbf{u}_i, \boldsymbol{\mathcal{R}}_i\boldsymbol{\eta})_{\Omega_i} + \nu(\nabla\mathbf{u}_i, \nabla\boldsymbol{\mathcal{R}}_i\boldsymbol{\eta})_{\Omega_i} - (p_i, \nabla\cdot\boldsymbol{\mathcal{R}}_i\boldsymbol{\eta})_{\Omega_i} + ((\mathbf{w}\cdot\nabla)\mathbf{u}_i, \boldsymbol{\mathcal{R}}_i\boldsymbol{\eta})_{\Omega_i}] \\ &= \sum_{i=1}^{2} [(\mathbf{f}, \mathbf{z}_i)_{\Omega_i} + (\mathbf{f}, \boldsymbol{\mathcal{R}}_i\boldsymbol{\eta})_{\Omega_i}] = (\mathbf{f}, \mathbf{v})_\Omega, \end{aligned} \tag{55}$$

thus $(\mathbf{u}, p)$ satisfy the momentum equation of (25).

Moreover, for any $q \in L^2(\Omega)$, $q_{|\Omega_i} \in L^2(\Omega_i)$, thus, by using $q_{|\Omega_i}$ as test functions in (45) we obtain

$$(\nabla\cdot\mathbf{u}, q)_\Omega = \sum_{i=1}^{2} (\nabla\cdot\mathbf{u}_i, q_{|\Omega_i})_{\Omega_i} = 0, \tag{56}$$

proving that $\mathbf{u}$ satisfies also the continuity equation. □

The following result, whose proof is similar to the proof of Theorem 3.3, is also valid.

Theorem 3.4. *Problem* (26) *is equivalent to the problem given by* (44), (45), (46), *and* (48), *while problem* (31) *is equivalent to the problem given by equations* (49), (45), (46) *and* (50), *in the sense that* $\mathbf{u}_{|\Omega_i} = \mathbf{u}_i$ *and* $p_{|\Omega_i} = p_i$ *for* $i = 1, 2$.

Remark 3.3. The multi-domain problem (41) may be solved by iterative substructuring methods (see [13], Ch. 3). In the current case, the idea consists of solving problems like (41) for every $i = 1, 2$, for which the transmission conditions (9) and (10) (or (11)) provide Dirichlet and friction boundary conditions on the interface Γ, respectively. This issue will be specifically addressed in [2] for the Navier–Stokes/Oseen coupling.

4. Test cases and numerical results

We aim at showing that, in certain situations, the coupled Navier–Stokes/Oseen model furnishes a good approximation to the full Navier–Stokes model. Moreover, we are interested in comparing the results that are obtained using the Oseen flux with those corresponding to the Stokes flux on the interface Γ of the decomposition.

From now on, the problem (44)–(47) is referred to as *Navier–Stokes/Oseen coupling with Stokes flux* on the interface, while the problem (49), (45), (46), (50) is referred to as *Navier–Stokes/Oseen coupling with Oseen flux* on the interface.

When comparing the coupled Navier–Stokes/Oseen (NS-O) solution with the solution (NS) of the full Navier–Stokes problem, the NS-O solution with Stokes flux is compared to the solution of (25), while the NS-O solution with Oseen flux is compared to the solution of (31).

A situation that we will consider is an exterior problem with "far-field" boundary conditions, i.e. $\mathbf{u}(\mathbf{x}) \to \mathbf{u}_\infty(\mathbf{x})$ as $\|\mathbf{x}\| \to \infty$, as in the study of the flow past a body (e.g., an aircraft). In this case the Navier–Stokes equations are used in the near field, while in the exterior domain the linear Oseen equations or the Stokes equations are solved.

Another case that we are going to consider is concerned with the fluid flow in a channel over a backward facing step, where Navier–Stokes equations are solved in the subdomain where the velocity is "high", whereas a simplified (linear) model is considered elsewhere.

The numerical approximation is carried out by considering either stabilised spectral elements (see [9], [8]) and finite elements.

As we have anticipated in Section 2.1, the non-linearity of the problem is gotten rid of by using the Euler semi-implicit scheme, so that, at each time-step, we face a heterogeneous Oseen/Oseen coupling. This coupled model is solved under a coercivity assumption such as (36), (37) or (40), as stated by Theorems 3.1 and 3.2).

However, being $\alpha = 1/\Delta t$, the condition (40) is always satisfied, thus the NS-O coupling with Oseen flux is always well defined.

On the other hand, the well posedness for formulation (25) (i.e. the Navier–Stokes/Oseen coupling with Stokes flux) is not guaranteed in all situations. In the

following test cases, however, the choice of the data α, $\mathbf{u}_\infty$ and $[\mathbf{w}]_\Gamma$ guarantees the existence of a unique solution.

4.1. Stationary 2D channel flow over a backward facing step

We have considered the domain of Figure 1 and the following data: a parabolic velocity profile (say $\mathbf{u}_{in}$) with maximum value equals to one at the inflow boundary; null Stokes flux at the outflow; no-slip conditions at fixed walls; viscosity: $\nu = 0.41\overline{6} \cdot 10^{-2}$, $0.208\overline{3} \cdot 10^{-2}$ or $0.1041\overline{6} \cdot 10^{-2}$. The corresponding Reynolds number, $Re = D\|\mathbf{u}_{in}\|/\nu$, is equal to 30, 60, and 120, respectively. The space discretisation is based on spectral elements with Galerkin–Least Squares stabilisation, with 32 elements, polynomial degree $N = 6$ in each element, for a total number of 3729 degrees of freedom. We have used also a spatial discretisation based on the finite element method, using $\mathbb{P}^1$ iso $\mathbb{P}^2$ elements for the velocity unknowns and $\mathbb{P}^1$ (continuous) elements for the pressure (see, [12]). The step size is $h = 0.02$.

The time discretisation is based on the Euler semi-implicit method with $\Delta t = 0.1$ for Spectral Elements and $\Delta t = 0.001$ for Finite Elements. The initial solution is $\mathbf{u}_0 = \mathbf{u}_{\text{Stokes}}$, that is the solution of the Stokes problem corresponding to the same data. For the above Reynolds numbers, the flow tends to a steady state.

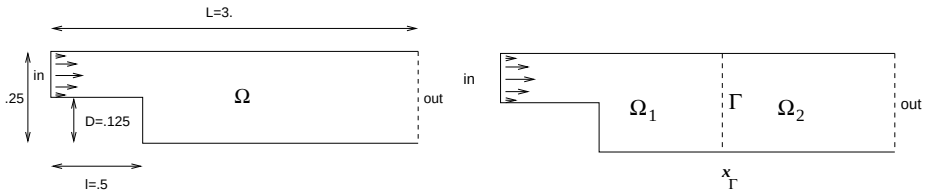

Fig. 1. The computational domain of the 2D channel flow over a backward facing step (left) an the decomposition of Ω for the heterogeneous coupling (right).

We solve the NS-O equations with either Stokes or Oseen flux with $\mathbf{u}_\infty = \mathbf{u}_{\text{Stokes}}$ on the decomposition indicated in Figure 1. Let us define the vector

$$\mathbf{x} = [1.25,\ 1.5,\ 1.75,\ 2.,\ 2.25,\ 2.5,\ 2.75]^t. \tag{57}$$

We denote by

$$\begin{array}{ll} (\mathbf{u}_{NS}, p_{NS}) & \text{the full NS solution in } \Omega, \\ (\mathbf{u}_i, p_i) & \text{the NS-O solution with interface } \Gamma \text{ such that} \\ & x_\Gamma = x_i,\ i = 1, 7, \\ (\mathbf{u}_0, p_0) & \text{the full NS solution in } \Omega_0 = \Omega \cap \{(x, y) :\ x \le 1.25\}. \end{array} \tag{58}$$

We define the relative errors by discrete H^1-norm:

$$e^i_{H^1(\Omega_0)} = \frac{\|\mathbf{u}_{NS} - \mathbf{u}_i\|_{H^1(\Omega_0)}}{\|\mathbf{u}_{NS}\|_{H^1(\Omega_0)}},\ i = 0, \ldots, 7 \tag{59}$$

and the sup norm of the jump on the interface:

$$s_i = \|[\mathbf{w}] \cdot \mathbf{n}\|_{L^\infty(\Gamma)}, \quad i = 1, \ldots, 7. \tag{60}$$

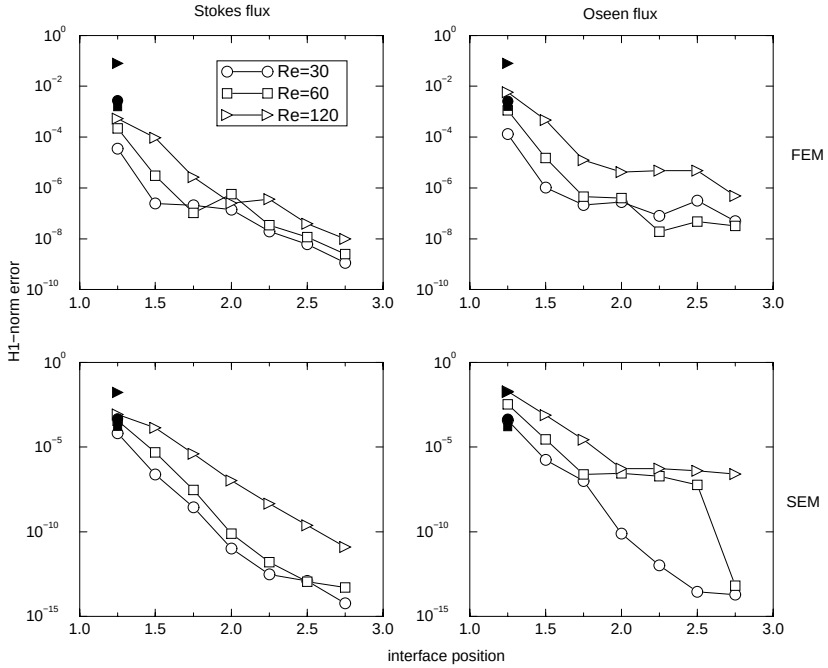

Fig. 2. The errors (59) for the problem of Section 4.1, with the Stokes flux (left) and the Oseen flux (right) on the interface and both Finite Elements (FEM) and Spectral Elements (SEM). The black symbols denote the error corresponding to the full NS solution in Ω_0. Different values of the interface position are considered.

When we use the skew-symmetric form of the convective term and, consequently, the Oseen flux across the interface, the natural boundary condition on the outflow boundary would be

$$T_O(\mathbf{w}; \mathbf{u}, p)\mathbf{n} = \mathbf{0}.$$

However, this condition gives rise to spurious oscillations on the velocity, so that it has been replaced by the condition of null Stokes flux at the outflow boundary, i.e.

$$T_S(\mathbf{u}, p)\mathbf{n} = \mathbf{0}. \tag{61}$$

In Figure 2 we show the behaviour of the errors $e^i_{H^1(\Omega_0)}$, versus x_Γ, the value of the interface abscissa, for both Finite Element methods and Spectral Element methods, while in Figure 3 we show the behaviour of the jump on the interface (60).

In Figure 4 we show the comparison between the solution of NS-O coupling (with either Oseen and Stokes flux) and that of the NS-S coupling, at $Re = 120$.

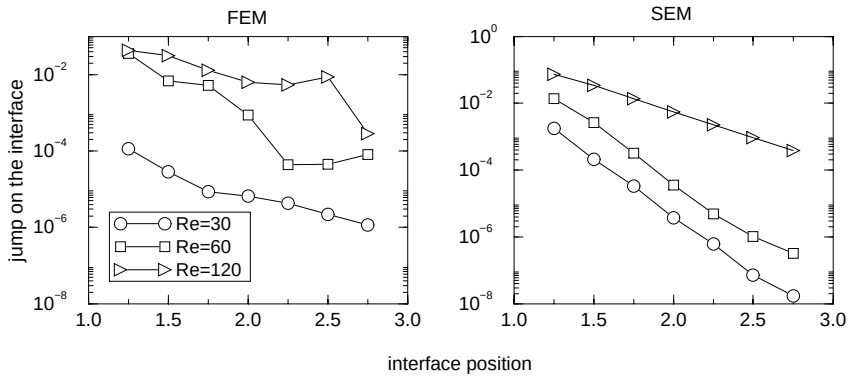

Fig. 3. The jump on the interface (60) for both FEM and SEM.

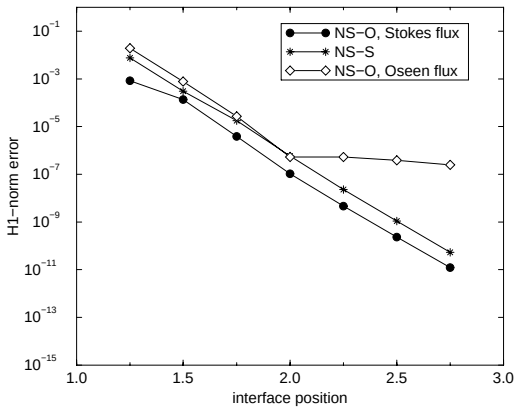

Fig. 4. The errors (59) for different values of the interface position for the problem of Section 4.1, at $Re = 120$ and null Stokes flux at the outflow boundary.

Finally, in Figures 5–10 we report the contour lines of the first component of the velocity and the contour lines of the pressure for several different coupling problems.

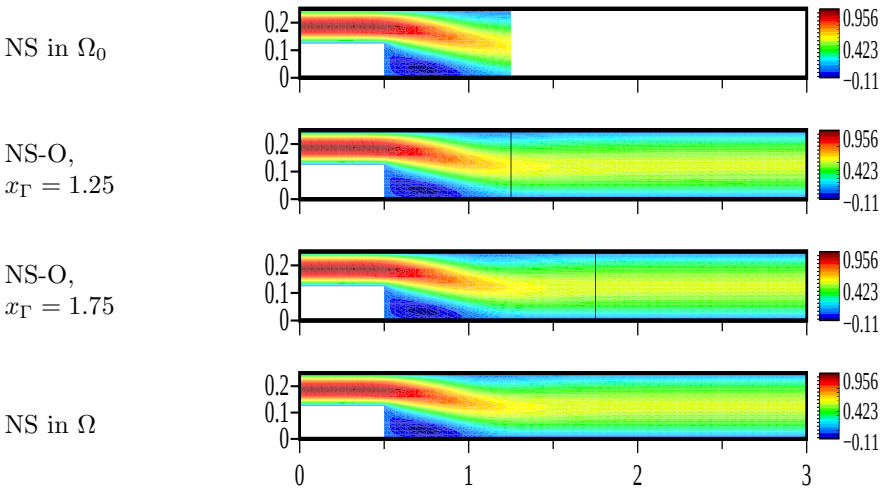

Fig. 5. Contour lines for the first component of the velocity, $Re = 120$, Stokes flux across the interface.

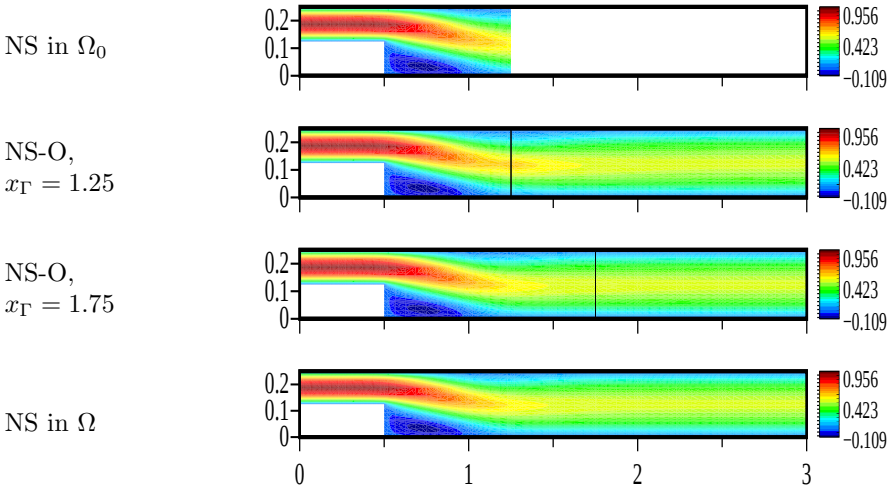

Fig. 6. Contour lines for the first component of the velocity, $Re = 120$, Oseen flux across the interface.

Remark 4.1. The numerical results show the convergence of the coupled NS-O and NS-S models to the full NS model when the interface position moves far from the recirculation zone. We observe that, when the Reynolds number gets large, the Stokes flux gives more accurate solutions than the Oseen flux. We point out that having positioned the interface behind the recirculation zone ensures the fulfilment of (36) for the coupling with Stokes flux.

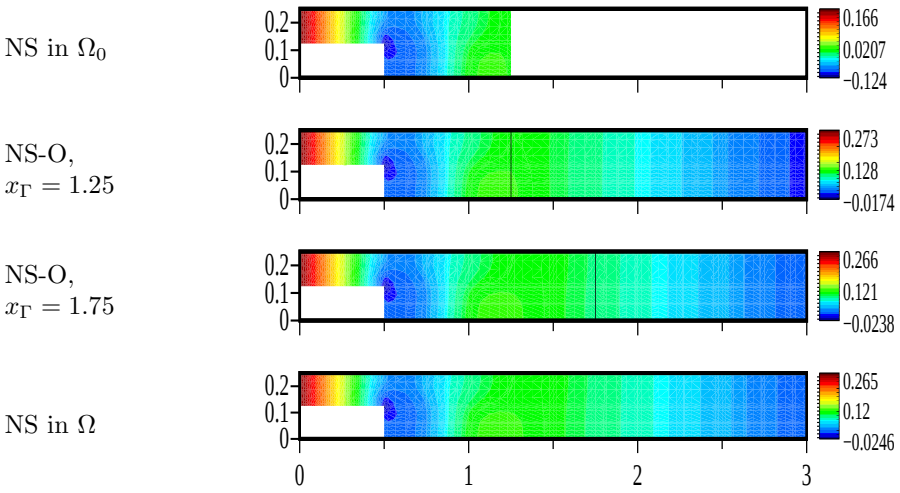

Fig. 7. Contour lines for the pressure, $Re = 120$, Stokes flux across the interface.

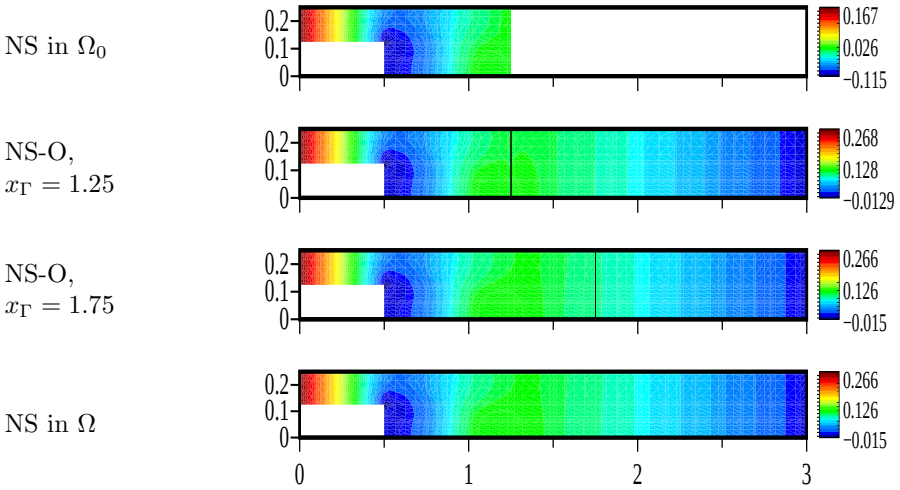

Fig. 8. Contour lines for the pressure, $Re = 120$, Oseen flux across the interface.

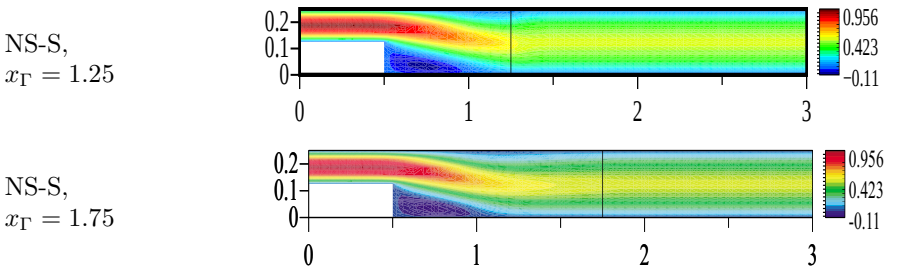

Fig. 9. Contour lines for the first component of the velocity, $Re = 120$, Stokes flux across the interface.

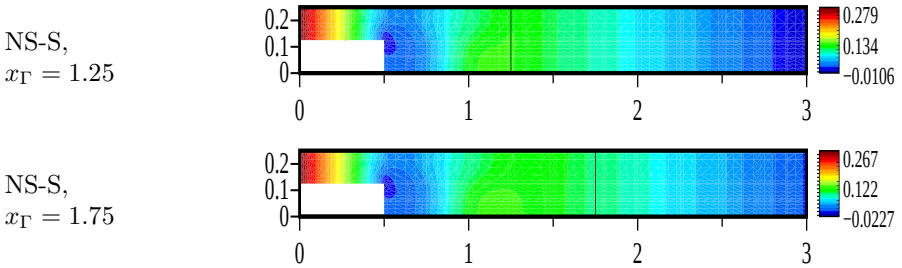

Fig. 10. Contour lines for the pressure, $Re = 120$, Stokes flux across the interface.

4.2. Flow around a cylinder

We consider now the motion of a fluid past a circular obstacle. The computational domain is $\Omega = (-4.5, 40.) \times (-4.59, 4.5)$ and the obstacle is a circle with diameter $D = 1$ (or $D = 2$), centred at $(0., 0.)$. The lack of symmetry on the geometry generates a periodic motion of the fluid (see [14]).

We have considered the domain of Figure 1 and the following data: $\mathbf{u}_\infty = [1, 0]^t$ on the inflow boundary; natural boundary conditions on the outflow; no-slip boundary conditions on the boundary of the cylinder, and slip boundary conditions on the horizontal sides. The viscosity is $\nu = 0.01$, so that the corresponding Reynolds number is 100 if $D = 1$, and 200 if $D = 2$. The space discretisation is based on spectral elements with Galerkin–Least Squares stabilisation, with 60 elements, polynomial degree $N = 5$ in each element, for a total number of 5115 degrees of freedom. The time discretisation is realized by Euler semi-implicit method with $\Delta t = 0.1$ and the initial solution is $\mathbf{u}_0 = \mathbf{u}_{\text{Stokes}}$, that is the solution of the Stokes problem corresponding to the same data.

For the NS-O coupling we have considered an interface located in x_i, with $i = 1, \ldots, 8$ and

$$\mathbf{x} = [6,\ 9,\ 12,\ 16,\ 20,\ 25,\ 30,\ 35]^t \tag{62}$$

and we have defined $\Omega_0 = \{(x, y) \in \Omega :\ x \leq 16\}$. The Stokes flux is imposed across the interface.

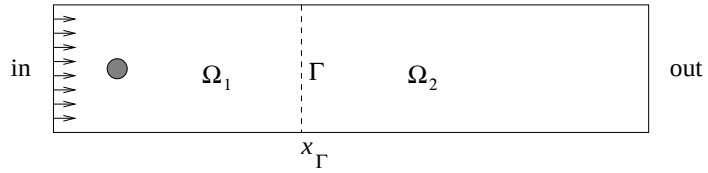

Fig. 11. The computational domain for the test case of Section 4.2.

The solution remains stable until the unsymmetry induced by the geometric imperfection is able to trigger the beginning of the vortex shedding. Next, a transient solution develops until the periodic solution is reached approximately at $t = 100$. When $Re = 100$ the period resulting is $T = 6.1\overline{3}$ (as we can observe from the graph of the drag and lift coefficients, Figure 12).

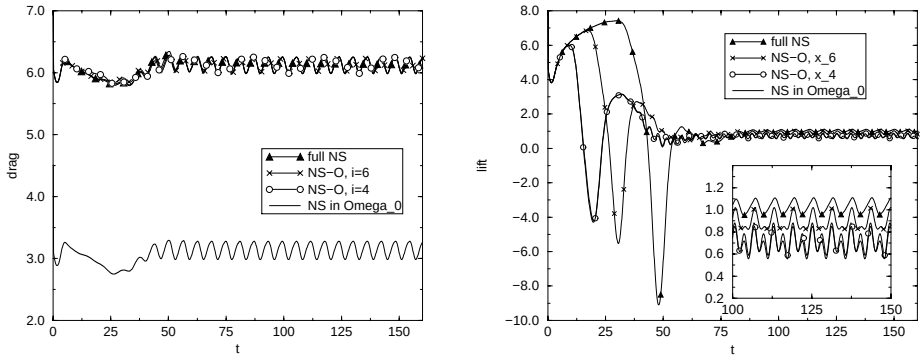

Fig. 12. Drag and lift coefficients corresponding to $D = 1$, $Re = 100$. The results refer to the full NS solution in Ω and in Ω_0 and to the NS-O coupling with $x_\Gamma = x_6 = 25$ and $x_\Gamma = x_4 = 16$.

We have approximated the full NS for $t \in [0, 160]$, and then we have solved the NS-O coupling for $t \in [130, 145]$ by taking $\mathbf{u}_\infty = [1, 0]^t$.

In Table 1 we report the errors $e^i_{H^1(\Omega_0)}$ versus the interface position at four different times.

	$t = 136$	$t = 139$	$t = 142$	$t = 145$
NS in Ω_0	2.85e-3	2.88e-3	2.88e-3	2.87e-3
NS-O with $x_\Gamma = 16$	1.52e-3	1.54e-3	1.52e-3	1.50e-3
NS-O with $x_\Gamma = 20$	2.33e-4	2.03e-4	1.74e-4	1.71e-4
NS-O with $x_\Gamma = 25$	5.85e-5	5.67e-5	5.05e-5	4.77e-5
NS-O with $x_\Gamma = 30$	1.03e-5	1.49e-5	1.43e-5	1.30e-5
NS-O with $x_\Gamma = 35$	2.02e-6	4.66e-6	5.96e-6	6.46e-6

Table 1. The H^1-norm errors (59) for the time-dependent problem with $Re = 100$ and $D = 1$. The coupled problem has been solved for $t \in [130, 145]$.

We note that, as for the test case of Section 4.1, the coupled NS-O model converges to the full NS model when the interface position moves far from the obstacle. Moreover, for every coupling, the error is independent of the time instant.

We have then solved the NS-O coupling with interface in $x_\Gamma = 25$ (corresponding to $i = 6$) and $x_\Gamma = 16$ ($i = 4$) and the full NS in Ω_0 for $t \in [0, 160]$. In Figure 13 we report the errors $e^i_{H^1(\Omega_0)}$ for $i = 0, 4, 6$ and $t \in [0, 160]$.

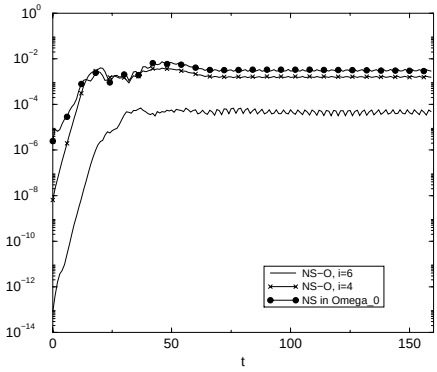

Fig. 13. Errors $e^i_{H^1(\Omega_0)}$ for the coupling NS-O and $i = 4, 6$ and for the full NS solution in Ω_0. $Re = 100$, $D = 1$.

Then, we have considered the same problem, but this time with $D = 2$, so that $Re = 200$. We have approximated the full NS for $t \in [0, 200]$ and we have solved the NS-O coupling for $t \in [180, 200]$ by taking $\mathbf{u}_\infty = [1, 0]^t$. In Table 2 we report the errors $e_{H^1,i}$ versus the interface position at two different time instants.

	$t = 190$	$t = 200$
NS in Ω_0	1.85e-2	1.67e-2
NS-O with $x_1 = 6$	1.42e-1	1.46e-1
NS-O with $x_2 = 9$	6.21e-2	6.53e-2
NS-O with $x_3 = 12$	3.41e-2	3.45e-2
NS-O with $x_4 = 16$	9.17e-3	8.16e-3
NS-O with $x_5 = 20$	6.85e-4	6.31e-4
NS-O with $x_6 = 25$	8.12e-5	9.56e-5
NS-O with $x_7 = 30$	1.27e-5	1.45e-5
NS-O with $x_8 = 35$	2.88e-6	3.41e-6

Table 2. $e^i_{H^1(\Omega_0)}$, for $i = 1, \ldots, 8$, for the time dependent problem with $Re = 200$ and $D = 2$. The coupling has been solved for $t \in [180, 200]$.

In the following figures (Figure 14–15) we report the contour lines of the first component of the velocity and the contour lines of the pressure for some couplings.

Remark 4.2. We observe that there is a good agreement between the velocity field of the coupled NS-O problem and the velocity field of the full NS problem when $x_\Gamma \geq 16$. As for the test case of Section 4.1, the "coercivity" for the problem (25) is satisfied, even when the interface is near the obstacle.

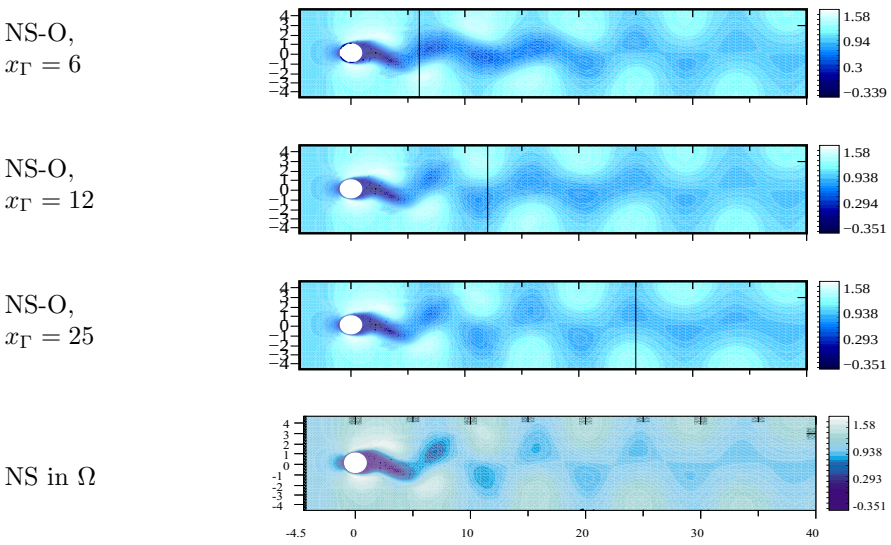

Fig. 14. Contour lines of the first component of the velocity at $t = 193$, $Re = 200$. Stokes flux across the interface and natural boundary conditions at the outflow boundary.

4.3. Flow around a cylinder in a circular domain

We consider now a circular domain of radius $R = 20$ with a circular obstacle of radius $R = 2$ in the middle of the domain (see Figure 16) and the following data: inflow boundary conditions $\mathbf{u}_\infty = [1/\sqrt{2}, 1/\sqrt{2}]^t$ on the subset of the external boundary where $\mathbf{u}_\infty \cdot \mathbf{n} < 0$; natural boundary conditions on the subset of the external boundary where $\mathbf{u}_\infty \cdot \mathbf{n} \geq 0$, no-slip boundary conditions on the cylinder boundary; viscosity: $\nu = 0.02$ (the corresponding Reynolds number is 100). We have used spectral elements with Galerkin–Least Squares stabilisation, with 60 elements and polynomial degree $N = 6$ in each element. The corresponding degrees of freedom are 6660. The time discretisation is employed by the Euler semi-implicit scheme with $\Delta t = 0.1$ and the initial condition at $t = 0$ is $\mathbf{u}_0 = \mathbf{u}_\infty$.

The NS-O coupling is realized imposing the Stokes flux across the interface; we have considered two possible decompositions, as shown in Figure 16.

As above, $(\mathbf{u}_{NS}, p_{NS})$ denotes the full NS solution in Ω, while $(\mathbf{u}_O, p_O)$ represents the NS-O solution.

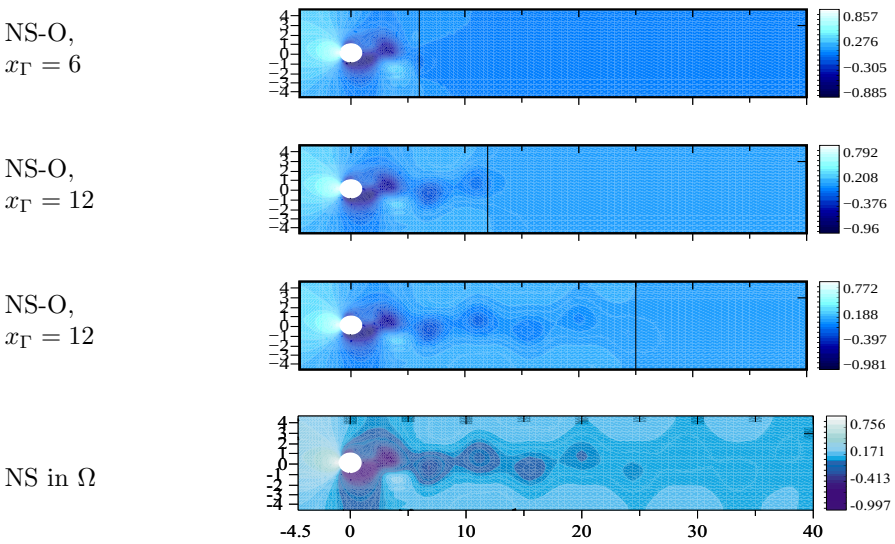

Fig. 15. Contour lines of the pressure at $t = 193$, $Re = 200$. Stokes flux across the interface and natural boundary conditions at the outflow boundary.

We consider the following error

$$e_{H^1(\Omega_1)} = \frac{\|\mathbf{u}_{NS} - \mathbf{u}_O\|_{H^1(\Omega_1)}}{\|\mathbf{u}_{NS}\|_{H^1(\Omega_1)}} \tag{63}$$

being Ω_1 the Navier–Stokes domain. The relative error (63) for the NS-O coupling solved in the time interval [0,330] are reported in Figure 17.

Finally we report the streamfunctions at time $t = 250$.

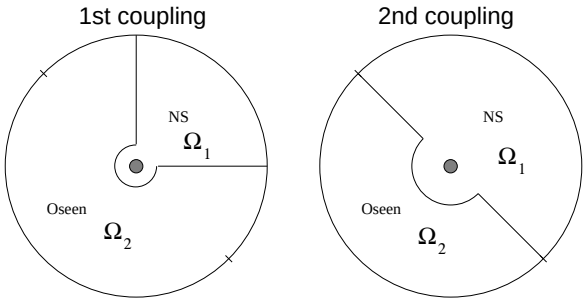

Fig. 16. The two decompositions used for the test case of Section 4.3.

We observe that the numerical solution of the first coupling is more accurate than the second one. For both type of couplings the problem (25) is still "coercive", thanks to the presence of the term $\alpha\|\mathbf{u}\|^2_{L^2(\Omega)}$.

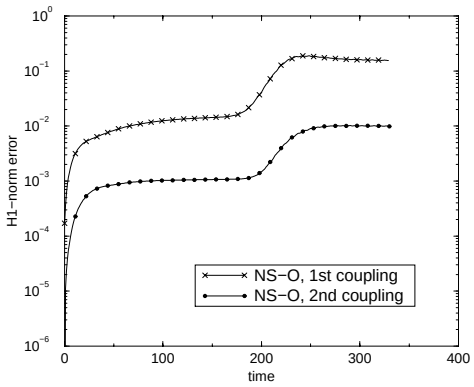

Fig. 17. The H^1-norm relative errors for the two NS-O coupling illustrated in Figure 16.

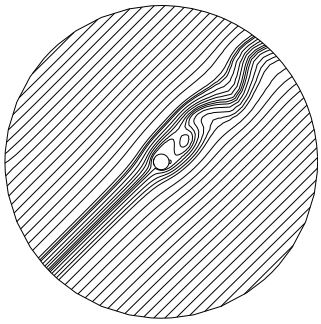

Fig. 18. The streamfunctions at $t = 250$ for the full NS solution. $Re = 100$.

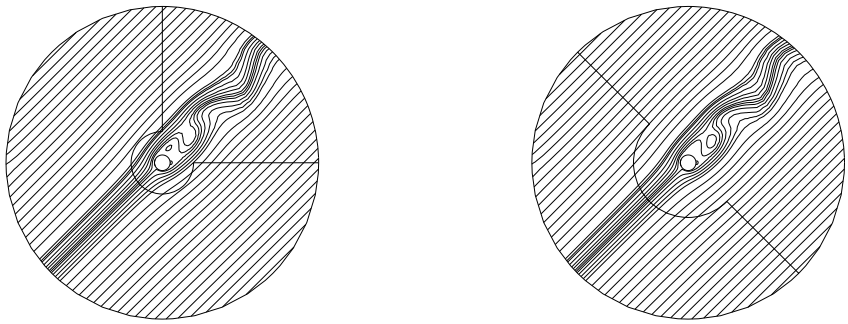

Fig. 19. The streamfunctions at $t = 250$ for the first (left) and second (right) NS-O coupling. $Re = 100$.

5. Conclusions

In this paper we have considered heterogeneous models that couple the Navier–Stokes equations with a simplified system that can be reasonably adopted in a given subregion of the computational domain.

We have proposed and analysed the conditions of continuity for the two solutions at subdomain interface, generalising previous results by Feistauer and Schwab.

The proposed models have then been validated and assessed on three different test cases of physical interest: steady flow in a channel with a backward facing step, unsteady flow past a cylinder in a channel, and unsteady flow past a cylinder in a circular domain.

The results show, from one hand, the correctness of our heterogeneous mathematical models. From the other hand, they clearly indicate the potential interest of using simplified models in subregions, according to a design principle that depends on the specific class of problems at hand.

As of computational efficiency, the numerical treatment of the coupled problems by suitable subdomain iterative methods is in order. This issue will be addressed in a forthcoming report [2].

Acknowledgements. We thank Prof. A. Valli for fruitful discussions during the preparation of this report. We also thank Dr. A. Veneziani for having provided a preliminary version of the FEM code.

References

[1] F. Brezzi and G. Gilardi, Functional analysis & Functional spaces, in: H. Kardestuncer (ed.), *Finite Element Handbook*, Chapters 1, 2, McGraw-Hill, New-York, 1987.

[2] L. Fatone, P. Gervasio and A. Quarteroni, Multimodels for incompressible flows: iterative solutions for the Navier–Stokes/Oseen coupling, Technical Report, in preparation, 2000.

[3] M. Feistauer and C. Schwab, Coupling of an interior Navier–Stokes problem with an exterior Oseen problem, Technical Report Research 98-01, ETH, Zürich, 1998.

[4] M. Feistauer and C. Schwab, On coupled problems for viscous flow in exterior domains, *Math. Models Methods Appl. Sci.* **8** (1998), 657–684.

[5] M. Feistauer and C. Schwab, Coupled problems for viscous incompressible flow in exterior domains, Technical Report Research 99-07, ETH, Zürich, 1999.

[6] G. P. Galdi, *An Introduction to the Mathematical Theory of the Navier–Stokes Equations. Vol. I. Linearized steady problems*, Springer Tracts in Natural Philosophy, 38, Springer-Verlag, New York, 1994.

[7] G. P. Galdi, *An Introduction to the Mathematical Theory of the Navier–Stokes Equations. Vol. II. Nonlinear steady problems*, Springer Tracts in Natural Philosophy, 39, Springer-Verlag, New York, 1994.

[8] P. Gervasio, A. Quarteroni and F. Saleri, Spectral Approximation of Navier–Stokes Equations, Technical report, Università degli Studi di Milano, quad. n. 31, 1998. To appear in the book P. Galdi, J. Heywood and R. Rannacher (Eds.), *Aspects of Mathematical Fluid Mechanics*, Birkhäuser, Basel, 2000.

[9] P. Gervasio and F. Saleri, Stabilized spectral element approximation for the Navier–Stokes equations, *Numerical Methods for Partial Differential Equations*, **14** (1998), 115–141.
[10] J. L. Lions and E. Magenes, *Nonhomogeneous Boundary Value Problems and Applications*, Springer Verlag, Berlin, 1972.
[11] P. L. Lions, *Mathematical topics in fluid mechanics. Vol. 1. Incompressible models*, Oxford Lecture Series in Mathematics and its Applications, 3. Oxford Science Publications. The Clarendon Press, Oxford University Press, New York, 1996.
[12] A. Quarteroni and A. Valli, *Numerical Approximation of Partial Differential Equations*, Springer Verlag, Heidelberg, 1994.
[13] A. Quarteroni and A. Valli, *Domain Decomposition Methods for Partial Differential Equations*, Oxford Science Publications, 1999.
[14] J. C. Simo and F. Armero, Unconditional stability and long-term behaviour of transient algorithms for the incompressible Navier–Stokes and Euler equations, *Comp. Meth. Appl. Mech. Engrg.* **111** (1992), 111–154.
[15] R. Temam, *Navier–Stokes Equations and Nonlinear Functional Analysis*, SIAM, Philadelphia, 1983.

L. Fatone
Department of Mathematics
Politecnico di Milano
Milano
Italy

and

Department of Mathematics
EPFL, Lausanne
Switzerland
e-mail: lorella.fatone@epfl.ch

A. Quarteroni
Department of Mathematics
EPFL, Lausanne
Switzerland

and

Department of Mathematics
Politecnico di Milano
Milano
Italy
e-mail: alfio.quarteroni@epfl.ch

P. Gervasio
Department of Mathematics
University of Brescia
Brescia
Italy
e-mail: gervasio@bsing.ing.unibs.it

(accepted: October 10, 1999)